Available online at www.sciencedirect.com
SCIENCE DIRECT®
Journal of Molecular Catalysis A: Chemical 233 (2005) 17–27
JOURNAL OF MOLECULAR CATALYSIS A: CHEMICAL
www.elsevier.com/locate/molcata

Pd catalyzed Heck reaction with the catalytic system $[Pd(Ph_2PC_6H_4\text{-}2\text{-}(CH_2NMe_2))(SR_F)_2]$ Examination of the electronic effects of fluorinated thiolates

Jaime G. Fierro-Arias [a], Rocío Redón [b], Juventino J. García [c], Simón Hernández-Ortega [a], Rubén A. Toscano [a], David Morales-Morales [a,*]

[a] *Instituto de Química, Universidad Nacional Autónoma de México, Cd. Universitaria, Circuito Exterior, Coyoacán, 04510 México D.F., Mexico*
[b] *Centro de Ciencias Aplicadas y Desarrollo Tecnológico (CCADET), Universidad Nacional Autónoma de México, Cd. Universitaria, Circuito Exterior, Coyoacán, 04510 México D.F., Mexico*
[c] *Facultad de Química, Universidad Nacional Autónoma de México, Cd. Universitaria, Circuito Exterior, Coyoacán, 04510 México D.F., Mexico*

Received 23 November 2004; received in revised form 29 January 2005; accepted 1 February 2005

Abstract

A series of palladium thiolate complexes of the $[Pd(Ph_2PC_6H_4\text{-}2\text{-}(CH_2NMe_2))(SR_F)_2]$ type have been synthesized in good yields by metathetical reactions of $[Pd(Ph_2PC_6H_4\text{-}2\text{-}(CH_2NMe_2))Cl_2]$ (**1**) with $[Pb(SR_F)_2]$, ($SR_F = {}^-SC_6F_5$, ${}^-SC_6F_4$-4-H, ${}^-SC_6H_4$-2-CF_3, ${}^-SC_6H_4$-4-F, ${}^-SC_6H_4$-2-F) and their crystal structures determined. Heck coupling reactions were carried out using $[Pd(Ph_2PC_6H_4\text{-}2\text{-}(CH_2NMe_2))(SR_F)_2]$, $SR_F = {}^-SC_6F_5$ (**2**), ${}^-SC_6F_4$-4-H (**3**), ${}^-SC_6H_4$-2-CF_3 (**4**), ${}^-SC_6H_4$-4-F (**5**), ${}^-SC_6H_4$-2-F (**6**) complexes as catalysts in order to examine the effect of the thiolates in the reaction of bromobenzene and styrene. The results obtained indicate that the less electron-withdrawing substituents on the thiolate moiety may favor higher yields in the Pd catalyzed Heck reaction using $[Pd(Ph_2PC_6H_4\text{-}2\text{-}(CH_2NMe_2))(SR_F)_2]$ as catalysts.

Keywords: P–N ligand; Hemilability; Heck reaction; C–C coupling reactions; Fluorinated thiolate complexes; Palladium complexes; Crystal structures; Catalysis

1. Introduction

Transition metal catalyzed reactions have acquired a fundamental roll in the modern organic chemistry [1]. Among them, palladium catalyzed C–C coupling reactions have been recognized as power tools in multiple organic transformations, from these the Heck reaction has been denominated as angular stone in modern organic synthesis [2]. This reaction consists in the coupling of a halo compound with a double bond. The importance of this reaction has transcended its potential applications in the laboratory, to become the main interest to scale these processes to an industrial level [3]. In the same way, the different catalysts employed to carry out this reaction have also evolved to achieve a better understanding of the factors affecting activity, selectivity and stability. In this sense, in recent years, several groups have been involved in the design of ligands able to afford robust catalysts, capable to withstand reaction conditions and oxidant atmosphere, which favor Heck couplings in an efficient manner with cheap reagent grade starting materials. From all the compounds employed so far, it seems like hemilabile hybrid ligands may offer an interesting option to carry out this process [4]. Moreover, the presence of these ligands in the coordination sphere of transition metal complexes may render interesting behaviors in solution as these ligands can be capable of full or partial de-ligation (hemilability) [4], being able to provide important extra coordination sites for incoming substrates during a catalytic process [4]. In addition, platinum group metal complexes containing thiolate ligands on its structure are rare [5], due in part to the well known tendency of these complexes

* Corresponding author. Tel.: +52 5556224514; fax: +52 5556162217.
E-mail address: damor@servidor.unam.mx (D. Morales-Morales).

1381-1169/$ – see front matter © 2005 Elsevier B.V. All rights reserved.
doi:10.1016/j.molcata.2005.02.007

to polymerize [6], affording in most of the cases intractable solids useless as potential catalysts in homogeneous catalysis. Usually, compounds containing sulfur on its structure have been neglected as potential homogeneous catalysts due to the extended belief of sulfur to be a catalyst poison. Thus, given our continuous interest in the design and synthesis of active and robust complexes for their employment as potential catalysts in industrial relevant transformations [7], we would like to report here the use of the P–N ligand [$Ph_2PC_6H_4$-2-(CH_2NMe_2)] as a stabilizing ligand and fluorinated thiolates as substituents for the fine tuning of the electronics in the synthesis of a series of palladium(II) complexes of the type [Pd($Ph_2PC_6H_4$-2-(CH_2NMe_2))(SR_F)$_2$]. The identification of the electronic effects of the different fluorinated thiolates over the reactivity of these palladium complexes in the Heck catalytic reaction of bromobenzene and styrene will be discussed.

2. Results and discussion

P–N ligand [$Ph_2PC_6H_4$-2-(CH_2NMe_2)], was conveniently synthesized by direct *ortho*-lithiation of *N*,*N*′-dimethylbenzylamine with *n*-BuLi and further treatment of the resulting *ortho*-lithiated species with diphenylchlorophosphine (PPh_2Cl) (Scheme 1).

This compound exhibits signals in the ^{1}H NMR spectra due to the presence of the aromatic protons at 6.89–7.32 ppm, and two singlets at 3.62 and 2.08 ppm due the presence of the CH_2 and CH_3 groups respectively. ^{31}P NMR analysis reveal a single peak in the NMR spectra at −14.78 ppm, from these analyses it was determined that the ligand had been obtained with enough purity to be used without further purification. Thus, reaction of the P–N ligand (1 equiv.) with one equivalent of the palladium starting material [Pd(COD)Cl_2] afforded complex [Pd($Ph_2PC_6H_4$-2-(CH_2NMe_2))Cl_2] (**1**) as a yellow microcrystalline powder in good yield. This compound exhibited similar ^{1}H NMR spectra as that of the free ligand, with signals due to the presence of the aromatic protons between 6.3 and 7.9 ppm. Signals corresponding to the CH_2 and CH_3 groups were identified at 3.1–3.7 and 2.8 ppm respectively. It is noteworthy that both these signals are broad, this being probably due to a dynamic process of the ligand once coordinated to the metal as shown in Scheme 2.

In fact, further analyses of the ^{1}H NMR spectra at low temperature (233 K) for complex **3** confirms this hypothesis, showing clear and very well defined signals for the CH_2 and CH_3 groups (Fig. 1), with two signals for the methylenic protons and two more for the methyl groups, thus confirming

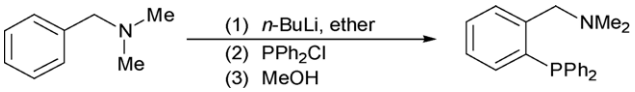

Scheme 1.

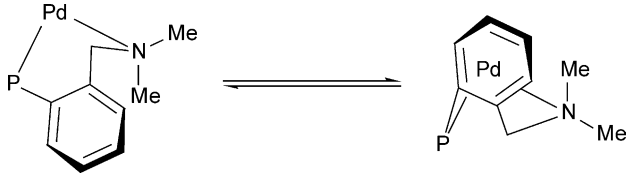

Scheme 2.

the magnetic inequivalence of these protons. The multiplicity of the signals for the protons of the CH_2 groups is due to the coupling between the protons themselves and given the closeness that one of the protons keeps at a given time with the P atom one of the signals is shown as a quartet. The other signals in the spectrum, may account for the presence of the other species in solution.

Analysis by ^{31}P NMR reveals a single peak, at lower field (22.9 ppm) clearly indicating that P moiety of the ligand is coordinated to the metal center. Analysis by MS-FAB+ spectrometry exhibits a peak corresponding to loss of a chloride $[M - Cl]^+$.

The stoichiometric reaction of the lead salt of the corresponding thiolate [Pb(SR_F)$_2$] with complex (**1**) afforded complexes **2**–**6** in good yields. All compounds were obtained as analytically pure products from recrystallization of CH_2Cl_2/MeOH solvent systems. Given the similarity in the structures of these complexes, common features in their spectroscopic properties were found. Analysis from the ^{1}H NMR of the series of complexes reveals a similar behavior as that observed for complex (**1**) with signals corresponding to the aromatic rings between 6.6 and 8.2 ppm and those corresponding to the methylene and methyl groups between 3.1 and 4.2 and about 2.87 ppm respectively, the fact that in all cases the signals for the CH_2 and CH_3 groups are broad once again indicate the presence of a dynamic equilibrium in solution. The ^{31}P{^{1}H} NMR spectra of the compounds are also very illustrative affording in all cases single resonances indicative of the presence of a single specie; another important feature in these spectra is that the signals observed are sensitive to the electronic environment, as expected, due to the number and position of the fluorine atoms in the aromatic rings of the thiolates. Thus, in the case of [Pd($Ph_2PC_6H_4$-2-(CH_2NMe_2))(SC_6F_5)$_2$] (**2**) the signal is shifted to lower field (δ = 20.88 ppm) and in the case of [Pd($Ph_2PC_6H_4$-2-(CH_2NMe_2))(SC_6H_4-2-CF_3)$_2$] (**4**) the signal is displaced to higher field (δ = 19.57 ppm); these two examples represent the upper and lower limits in the series of complexes. This behavior can be rationalized from the point of view of electron-withdrawing capability, being higher in the case of complex **2** due to the higher substitution of fluorine of the aromatic ring, and therefore, with the larger value of Group Electronegativity (Eg) [8], having the dishielding of the P nuclei in the P–N moiety as ultimate consequence. Thus, the trend observed for the δ ^{31}P{^{1}H} in the series of complexes [Pd($Ph_2PC_6H_4$-2-(CH_2NMe_2))(SR_F)$_2$] is: $^-SC_6H_4$-2-CF_3 (19.57 ppm) < $^-SC_6H_4$-4-F (20.35 ppm) < $^-SC_6H_4$-2-

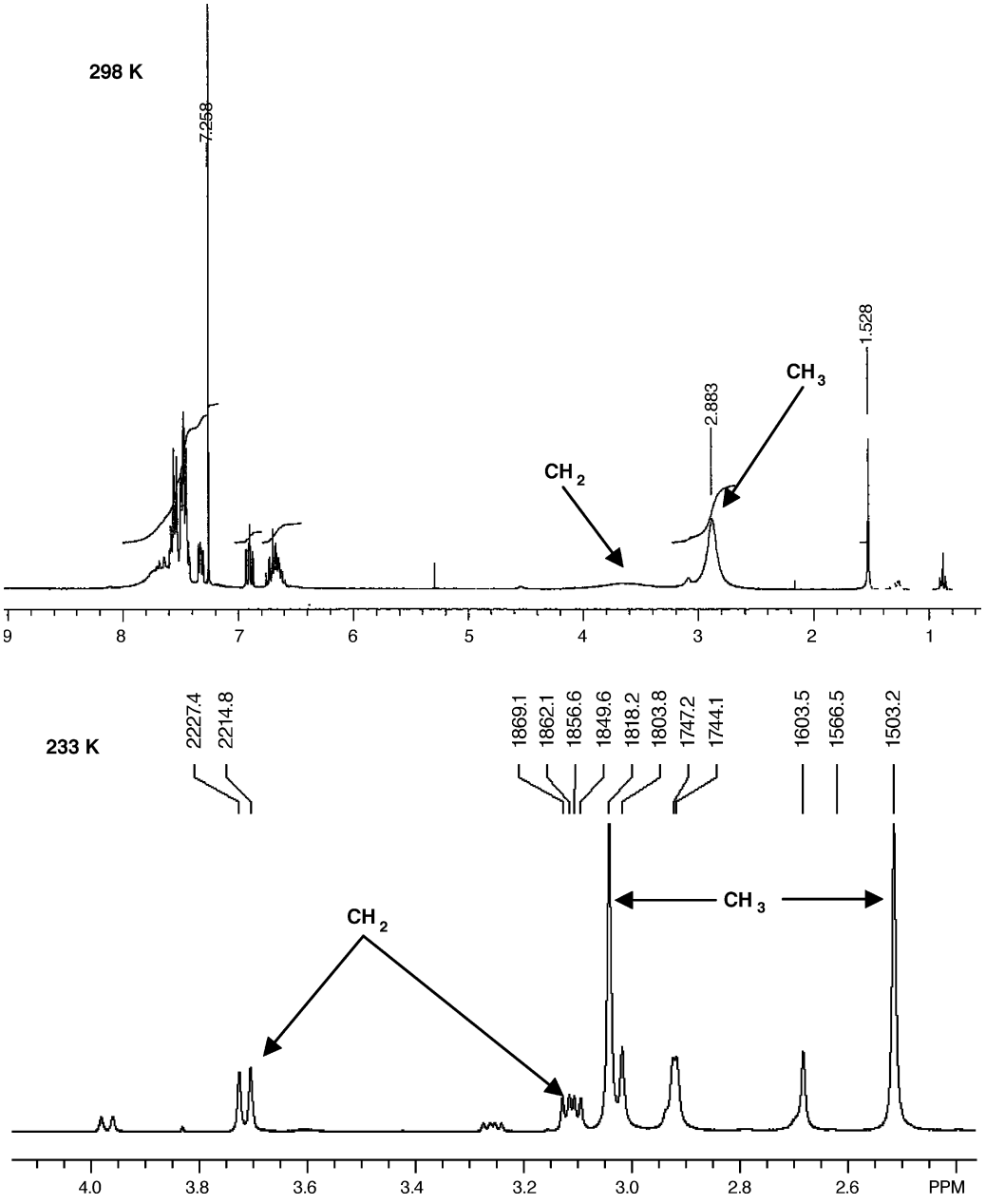

Fig. 1. ^{1}H NMR spectra for complex [Pd($Ph_2PC_6H_4$-2-(CH_2NMe_2))(SC_6F_4-4-H)$_2$] (**3**) at 298 and 233 K.

F (20.57 ppm) < $^{-}SC_6F_4$-4-H (20.88 ppm) < $^{-}SC_6F_5$ (20.97 ppm).

On the other hand, the $^{19}F\{^{1}H\}$ NMR experiments of the synthesized complexes reveal the fluorinated thiolates to be present, with typical splitting patterns for the ligands $^{-}SC_6F_5$ (**2**) and $^{-}SC_6F_4$-4-H (**3**) and singlets for the cases $^{-}SC_6H_4$-2-CF_3 (**4**), $^{-}SC_6H_4$-4-F (**5**) and $^{-}SC_6H_4$-2-F (**6**). These observed patterns are in agreement with the proposed formulations. In all cases the signals are duplicated, this being due to the fact that the fluorines are not equivalent since one thiolate has a phosphorus *trans* to it and the other one has the amino group in the *trans* conformation. Additionally, analysis by FAB^{+}-mass spectrometry shows in all cases the molecular ion of the fragment corresponding to the loss of one thiolate ligand. Further loss of the other thiolate ligand and a methyl fragment from the NMe_2 moiety were also observed. Elemental analyses for all the complexes are consistent with the proposed formulations.

Crystals suitable for single crystal X-ray diffraction analyses (Table 1) were obtained for complexes **1**, **3** and **4** and a rather unusual specie having a single thiolate in the coordination sphere [Pd($Ph_2PC_6H_4$-2-(CH_2NMe_2))(Cl)(SC_6H_4-2-F)] (**7**), this compound was obtained in minimum amount as by-product of the reaction for the synthesis of complex **6**. Once again these compounds share a number of common structural features. The structures can be defined as slightly

Table 1
Summary of crystal structure data for [Pd(P–N)$(SR_F)_2$] R = Cl (**1**), C_6F_4-4-H (**3**), C_6H_4-4-CF_3 (**4**), (Cl)(C_6H_4-2-F) (**7**)

Compound	[Pd(P–N)$(Cl)_2$] (**1**)	[Pd(P–N)$(SC_6F_4$-4-H$)_2$] (**3**)	[Pd(P–N)$(SC_6H_4$-2-$CF_3)_2$] (**4**)	[Pd(P–N)(Cl)$(SC_6H_4$-2-F$)_2$] (**7**)
Empirical formula	$C_{21}H_{22}Cl_2NPPd$	$C_{33}H_{24}F_8NPPdS_2$	$C_{35}H_{30}F_6NPPdS_2$	$C_{27}H_{26}ClFNPPdS$
Formula weight	496.67	788.02	780.09	588.37
Temperature (K)	293(2)	291(2)	291(2)	293(2)
Crystal system	Orthorhombic	Monoclinic	Monoclinic	Monoclinic
Space group	*Pbca*	$P2_1/c$	$P2_1/n$	$P2_1/c$
Crystal size (mm × mm × mm)	0.20 × 0.12 × 0.08	0.30 × 0.10 × 0.1	0.30 × 0.20 × 0.10	0.222 × 0.082 × 0.082
Unit cell dimensions				
a (Å)	15.642(1)	11.3895(6)	11.8450(9)	10.492(1)
b (Å)	14.820(1)	16.4315(8)	9.1040(7)	18.149(1)
c (Å)	18.226(1)	17.9115(9)	31.280(2)	14.211(1)
α (Å)	90	90	90	90
β (Å)	90	106.809(1)	97.906(2)	107.005(2)
γ (Å)	90	90	90	90
Volume ($Å^3$)	4224.9(3)	3208.9(3)	3341.1(4)	2587.7(3)
Z	8	4	4	4
Density (g/cm^3)	1.562	1.631	1.551	1.510
θ range for data collection (°)	2.20–25.00	1.87–25.00	1.77–25.00	1.87–32.59
Reflections collected	32875	25976	26646	35358
Independent reflections	3722 [*R*(int) = 0.0622]	5654 [*R*(int) = 0.0645]	5879 [*R*(int) = 0.0635]	9363 [*R*(int) = 0.1017]
F(0 0 0)	2000	1576	1576	1192
Absorption correction	Face-indexed	None	None	Analytical: face-indexed
Goodness-of-fit on F^2	1.027	0.965	0.956	0.972
R indices (all data)	$R_1 = 0.0485$, $wR_2 = 0.0463$	$R_1 = 0.0670$, $wR_2 = 0.0618$	$R_1 = 0.0742$, $wR_2 = 0.0856$	$R_1 = 0.2053$, $wR_2 = 0.0780$
Final *R* indices [$I > 2\sigma(I)$]	$R_1 = 0.0306$, $wR_2 = 0.0447$	$R_1 = 0.0424$, $wR_2 = 0.0586$	$R_1 = 0.0.0460$, $wR_2 = 0.0777$	$R_1 = 0.0569$, $wR_2 = 0.0644$
Data/restrains/parameters	3722/0/237	5654/0/417	5879/0/415	9363/0/300
Index ranges	$-18 \le k \le 18$, $-17 \le h \le 17$, $-21 \le l \le 21$	$-13 \le k \le 13$, $-19 \le h \le 19$, $-21 \le l \le 21$	$-14 \le k \le 14$, $-10 \le h \le 10$, $-37 \le l \le 37$	$-15 \le k \le 115$, $-27 \le h \le 27$, $-21 \le l \le 21$

$S = [w((F_o)^2 - (F_c)^2)^2/(n-p)]^{1/2}$ where n = number of reflections and p = total number of parameters. $R_1 = |F_o - F_c|/|F_o|$, $wR_2 = [w((F_o)^2 - (F_c)^2)^2/w(F_o)^2]$.

distorted square planar in all cases, having the palladium centers with the P–N ligand coordinated in a bidentate manner and completing the coordination sphere with the two thiolates adopting a *cis* conformation, one *trans* to one phosphorus and the other *trans* to the nitrogen of the P–N ligand. The main distortion is due to the steric hindrance caused by the phenyl rings in the P–N ligand. In all cases, the aromatic rings of the thiolates are not eclipsed as has been observed in other cases due to π–π interactions [9]. Instead, the aromatic rings are shifted, in an *anti* configuration. It is probable that the fluorobenzene rings adopt this conformation due to steric hindrance or to have optimal packing in the lattice.

In addition, analyses of the bond distances of the substituents *trans* to P and N in the series of complexes, reveal that the more elongated distance is that corresponding to the substituents *trans* to P. Therefore, one would expect the substitution of this ligand to proceed more easily than that of the ligand *trans* to N (e.g. for complex **1** *trans* to P Pd(1)–Cl(1) 2. 3903 (9) > *trans* to N Pd(1)–Cl(2) 2.2786 (9)). In fact, the *trans* influence of the phosphine is bigger than that of the amino group ($PR_3 > R_2N$). However complex **6** is obtained with the thiolate ligand *trans* to N, thus it seems that the ruling factors in the substitution of the chlorides in complex **1**, are the kinetic and not thermodynamic ones.

The differences observed, particularly in the $^{31}P\{^1H\}$ NMR experiments, are complemented with the results obtained from single crystal X-ray diffraction experiments. Although we cannot make a complete comparison due to the fact that we do not have the whole set of complexes crystallographically characterized, we can compare the two examples (complexes **3** and **4**) that represent extremes in the series. Thus, the differences in changing the thiolates are very clear. For instance, the Pd–S bond lengths (Table 2) decrease as the value of the Eg increases. This is most likely the result of either steric hindrance or electrostatic repulsion phenomena.

We believe that we have an ideal system to evaluate the importance of the fine tuning of the electronic effects in the palladium catalyzed Heck reaction. Thus, catalytic experiments were carried out employing [Pd($Ph_2PC_6H_4$-2-(CH_2NMe_2))($SR_F)_2$] complexes as catalysts. The reactions of bromobenzene and styrene using *N*,*N*-dimethylformamide (DMF) as solvent were carried out in the open air at different reaction times, revealing that 2 h of reaction time would yield enough product (stilbenes) to observe a clear trend to be able to quantify the effects due to the variation of the Eg of the thiolates. Given the fact that single substituted thiolates in different positions of the aromatic ring were also employed, some insights with respect to the sterics can also be obtained Table 3.

Table 2
Selected bond lengths (Å) and angles (°) for [Pd(P–N)(SR_F)$_2$], R = C_6F_4-4-H (**3**), C_6H_4-4-CF_3 (**4**), C_6H_4-2-F (**7**)

[Pd(P–N)(Cl)$_2$] (**1**)		[Pd(P–N)(SC_6F_4-4-H)$_2$] (**3**)		[Pd(P–N)(SC_6H_4-2-CF_3)$_2$] (**4**)		[Pd(P–N)(Cl)(SC_6H_4-2-F)] (**7**)	
Bond length (Å)							
Pd(1)–N(1)	2.110(2)	Pd(1)–N(1)	2.174(3)	Pd(1)–N(1)	2.161(3)	Pd(1)–N(1)	2.166(3)
Pd(1)–P(2)	2.2240(9)	Pd(1)–P(1)	2.2618(11)	Pd(1)–P(1)	2.2634(11)	Pd(1)–P(1)	2.2232(12)
Pd(1)–Cl(2)	2.2786(9)	Pd(1)–S(1)	2.2851(11)	Pd(1)–S(1)	2.2983(11)	Pd(1)–S(1)	2.2935(12)
Pd(1)–Cl(1)	2.3903(9)	Pd(1)–S(2)	2.3659(11)	Pd(1)–S(2)	2.3830(11)	Pd(1)–Cl(1)	2.3803(12)
Bond angle (°)							
N(1)–Pd(1)–P(2)	92.02(8)	N(1)–Pd(1)–P(1)	91.67(8)	N(1)–Pd(1)–P(1)	92.94(10)	N(1)–Pd(1)–P(1)	91.97(10)
N(1)–Pd(1)–Cl(2)	173.13(8)	N(1)–Pd(1)–S(1)	174.06(8)	N(1)–Pd(1)–S(1)	170.13(10)	N(1)–Pd(1)–S(1)	173.05(12)
P(2)–Pd(1)–Cl(2)	88.19(3)	P(1)–Pd(1)–S(1)	85.66(4)	P(1)–Pd(1)–S(1)	84.48(4)	P(1)–Pd(1)–S(1)	85.28(5)
N(1)–Pd(1)–Cl(1)	91.26(8)	N(1)–Pd(1)–S(2)	88.05(8)	N(1)–Pd(1)–S(2)	88.35(10)	N(1)–Pd(1)–Cl(1)	90.95(10)
P(2)–Pd(1)–Cl(1)	175.50(3)	P(1)–Pd(1)–S(2)	174.17(4)	P(1)–Pd(1)–S(2)	176.57(4)	P(1)–Pd(1)–Cl(1)	171.71(5)
Cl(2)–Pd(1)–Cl(1)	88.93(4)	S(1)–Pd(1)–S(2)	95.15(4)	S(1)–Pd(1)–S(2)	94.77(4)	S(1)–Pd(1)–Cl(1)	92.65(5)

Table 3
Heck couplings of bromobenzene with [Pd($Ph_2PC_6H_4$-2-(CH_2NMe_2))(SR_F)$_2$], R = C_6F_5 (**2**), C_6F_4-4-H (**3**), C_6H_4-2-CF_3 (**4**), C_6H_4-4-F (**5**), C_6H_4-2-F (**6**) as catalyst

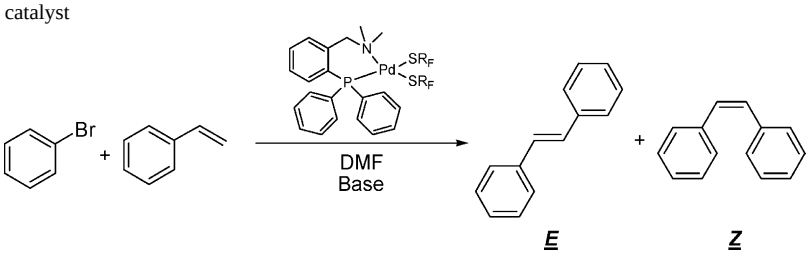

Entry	SR_F	Eg	% Conversion[a]
1	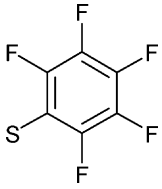	3.07	30.22
2	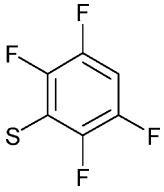	2.92	52.35
3	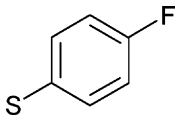	2.48	66.86
4	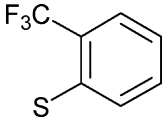	2.48	43.28
5	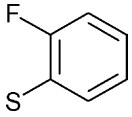	2.48	40.82

Reaction conditions 50 mmol of halobenzene, 60 mmol of styrene, 60 mmol of base, 4.0×10^{-5} mmol of catalyst and 5 mL of DMF, 2 h at 120 °C.
[a] Yields obtained by GC are based on bromobenzene.

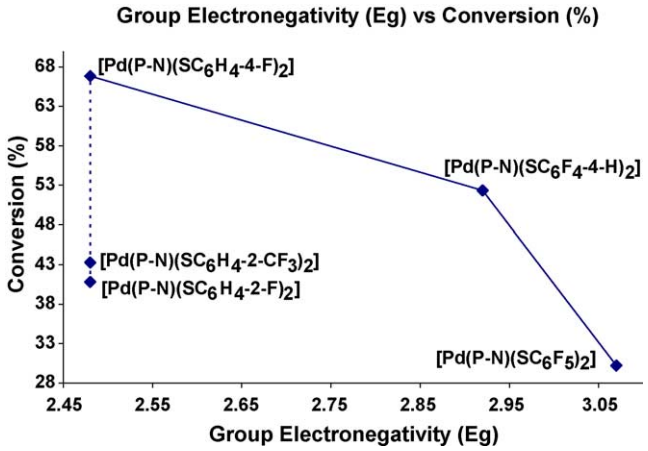

Fig. 2. Group Electronegativity (Eg) vs. conversion (%).

To better visualize the above-mentioned effects, graphics of the yield of stilbenes versus Group Electronegativity (Eg) (Fig. 2) were plotted. From this graphic, one can observe that as the Group Electronegativity (Eg) increases the yield of stilbenes decreases (solid line). However, from this figure it is not clear whether the position of the substituent in the aromatic ring of the thiolate plays an important role in the production of stilbenes (dotted line). Thus, although we have observed some variation in the catalytic performance of the complexes, at least in the present case, it is not clear whether sterics or electronics are important and this has to be investigated further, probably by employing bigger substituents in the aromatic ring of the thiolate. However, from the graphs it seems that a palladium system containing the P–N ligand and low electron-withdrawing substituents may lead to excellent catalysts for the high yield palladium catalyzed Heck reaction.

In summary, we have reported an efficient synthetic procedure for the synthesis of monomeric [Pd($Ph_2PC_6H_4$-2-(CH_2NMe_2))(SR_F)$_2$] complexes. These compounds have been evaluated in the palladium catalyzed Heck reaction of bromobenzene and styrene. Preliminary catalytic experiments indicate these complexes to be efficient catalyst in the Heck reaction. Analysis of the electronic effects of the thiolates on the performance of the different complexes reveal some variations, however, up to this point it remains unclear whether electronics or sterics are important. This preliminary data indicate (for complexes **1**, **2** and **3**) that as the value of Eg is increased, the total yield of stilbenes decreases, indicating that low electron-withdrawing substituents may favor higher yields in the Pd catalyzed Heck reaction using [Pd($Ph_2PC_6H_4$-2-(CH_2NMe_2))(SR_F)$_2$] as the catalytic system. Efforts aimed to employ these compounds in metal mediated organic syntheses and other C–C coupling reactions are currently under investigation.

From the results obtained it is clear that the different thiolate ligands affect the activity of the complexes in their catalytic performance, according to these results we believe that the mechanism involving these species may involve the partial dissociation of the P–N ligand and thus acting, as expected, as a hemilabile ligand, and thus generating the necessary coordination site for the incoming substrates to carry out the catalysis, at this point it results logic to think that these species may go through the accepted Pd(II)/Pd(0) mechanism given the well known tendency of sterically hindered thiolates to stabilize low coordination and oxidation states, thus different thiolate ligands may confer to the active catalytic species different stabilities or life times for the active species, this accounting for the different yields obtained at equal reaction times.

3. Experimental

3.1. Materials and methods

Unless stated otherwise, all reactions were carried out under an atmosphere of dinitrogen using conventional Schlenk glassware. Solvents were dried using established procedures and distilled under dinitrogen immediately prior to use. The IR spectra were recorded on a Nicolet-Magna 750 FT-IR spectrometer as nujol mulls. The ^{1}H NMR (300 MHz) spectra were recorded on a JEOL GX300 spectrometer. Chemical shifts are reported in ppm down field of TMS using the solvent ($CDCl_3$, $\delta = 7.27$) as an internal standard. $^{31}P\{^1H\}$ NMR (121 MHz) and $^{19}F\{^1H\}$ spectra were recorded with complete proton decoupling and are reported in ppm using 85% H_3PO_4 and C_6F_6 as external standards respectively. Elemental analyses were determined on a Perkin-Elmer 240. Positive-ion FAB mass spectra were recorded on a JEOL JMS-SX102A mass spectrometer operated at an accelerating voltage of 10 kV. Samples were desorbed from a nitrobenzyl alcohol (NOBA) matrix using 3 keV xenon atoms. Mass measurements in FAB are performed at a resolution of 3000 using magnetic field scans and the matrix ions as the reference material or, alternatively, by electric field scans with the sample peak bracketed by two (polyethylene glycol or cesium iodide) reference ions. GC–MS quantitative analyses were performed on a Varian Saturn 3 with a 30.0 m DB-5 capillary column. Melting points were determined in a MEL-TEMP capillary melting point apparatus and are reported without correction.

$PdCl_2$ was obtained commercially from Aldrich Chem. Co. Compounds [Pd(COD)Cl_2] [10], and [Pb(SR_F)$_2$] [11]; $R_F = C_6F_5$, C_6F_4-4-H, C_6H_4-2-CF_3, C_6H_4-4-F, C_6H_4-2-F were synthesized according to the published procedures.

3.2. Synthesis of the ligand [$Ph_2PC_6H_4$-2-(CH_2NMe_2)]

To a solution of $C_6H_5CH_2NMe_2$ (8.85 g, 0.07 mol) in ether (100 mL), a hexane solution of *n*-BuLi (45 ml of a 2.0 M, 0.9 mol) was added dropwise under stirring, the resulting orange solution was allowed to stand overnight at room temperature, after which time orange crystals were de-

posited. The mixture was then cooled to −78 °C on a dry ice/acetone bath and a solution of PPh_2Cl (13.0 g, 0.06 mol) in ether (100 mL) added dropwise. The mixture was then allowed to reach room temperature and stirred for one extra hour. After this time, ethanol (5 mL) and water (100 mL) were added to quench the reaction and the product extracted with ether (3 × 30 mL) and dried over sodium sulfate. Evaporation of the solvent afford a viscous oil that crystallizes with time. The product was analyzed by ^{31}P NMR showing the compound to be pure enough to be used without further purification. Yield 40% m.p. 54–56 °C. ^1H NMR (300 MHz, $CDCl_3$), δ 7.32–6.89 (m, Ph, 14H), 3.62 (s, CH_2, 2H), 2.08 (s, CH_3, 6H); $^{31}P\{^1H\}$ NMR (121 MHz, $CDCl_3$), δ −14.78 (s, P). Elem. Anal. Calculated for [$C_{21}H_{22}NP$] Calc. %—C: 78.97, H: 6.94. Found %—C: 78.94, H: 6.96. MS-FAB$^+$ [M^+] = 319 *m*/*z*.

3.3. Synthesis of [Pd($Ph_2PC_6H_4$-2-(CH_2NMe_2))Cl_2] (**1**)

To a solution of [Pd(COD)$(Cl)_2$] (153.6 mg, 0.47 mmol) in CH_2Cl_2 (15 ml), a solution of the P–N ligand [$Ph_2PC_6H_4$-2-(CH_2NMe_2)] (150 mg, 0.47 mmol) in CH_2Cl_2 (15 mL) was added dropwise under stirring, the resulting yellow solution was allowed to stir overnight, after which time the solution was filtered through a short plug of Celite® and the solvent removed under vacuum. The residue was recrystallized from CH_2Cl_2–pentane, to afford **1** as a yellow microcrystalline powder. Yield 95%. m.p. 150–151 °C. ^1H NMR (300 MHz, $CDCl_3$), δ 7.9–6.3 (m, Ph, 14H), 3.7–3.1 (br, s, CH_2, 2H), 2.8 (br, s, CH_3, 6H); $^{31}P\{^1H\}$ NMR (121 MHz, $CDCl_3$), δ 22.9 (s, P). Elem. Anal. Calculated for [$C_{21}H_{22}Cl_2NPPd$] Calc. %—C: 50.78, H: 4.46. Found %—C: 51.00, H: 4.42. MS-FAB$^+$ [M^+] = 497 *m*/*z*.

3.4. General procedure for the synthesis of the complexes [Pd($Ph_2PC_6H_4$-2-(CH_2NMe_2))(SR_F)$_2$]

All the complexes were obtained using the same experimental procedure. As a representative example, the synthesis of [Pd($Ph_2PC_6H_4$-2-(CH_2NMe_2))(SC_6F_5)$_2$] is described (Scheme 3).

3.4.1. Synthesis of [Pd($Ph_2PC_6H_4$-2-(CH_2NMe_2)) (SC_6F_5)$_2$] (**2**)

To a solution of [Pd($Ph_2PC_6H_4$-2-(CH_2NMe_2))Cl_2] (50 mg, 0.1 mmol) in acetone (20 mL), a solution of [Pb(SC_6F_5)$_2$] (60.7 mg, 0.1 mmol) in acetone (20 mL) was added dropwise under stirring, the resulting red-brick solution was allowed to stir overnight, after which time the solution was filtered through a short plug of Celite® and the solvent removed under vacuum. The residue was recrystallized from CH_2Cl_2–hexane, to afford **2** as a red microcrystalline powder. Yield 85.4%. m.p. 217–218 °C. ^1H NMR (300 MHz, $CDCl_3$), δ 8.2–6.8 (m, Ph, 14H), 4.2–3.1 (br, s, CH_2, 2H), 2.87 (br, s, CH_3, 6H); $^{31}P\{^1H\}$ NMR (121 MHz, $CDCl_3$), δ 20.97 (s, P); $^{19}F\{^1H\}$ NMR (282 MHz, $CDCl_3$), δ −134.6 (dd, $^3J_{Fo\text{-}Fm}$ = 22.01 Hz, *o*-F *trans* to N), −135.6 (dd, $^3J_{Fo\text{-}Fm}$ = 22.01 Hz, *o*-F *trans* to P), −163.0 (t, $^3J_{Fm\text{-}Fp}$ = 22.01 Hz, *p*-F *trans* to N), −164.5 (t, $^3J_{Fm\text{-}Fp}$ = 22.01 Hz, *p*-F *trans* to P), −166.2 (m, $^4J_{Fo\text{-}Fp}$ = 4.8, *m*-F *trans* to N), −166.8 (m, $^4J_{Fo\text{-}Fp}$ = 4.8, *m*-F *trans* to P). Elem. Anal. Calculated for [$C_{33}H_{22}F_{10}NPPdS_2$] Calc. %—C: 48.10, H: 2.69. Found %—C: 48.14, H: 2.68. MS-FAB$^+$ [M^+] = 822 *m*/*z*.

3.4.2. Synthesis of [Pd($Ph_2PC_6H_4$-2-(CH_2NMe_2)) (SC_6F_4-4-H)$_2$] (**2**)

[Pd($Ph_2PC_6H_4$-2-(CH_2NMe_2))Cl_2] (50.0 mg, 0.1 mmol) in acetone (20 mL), a solution of [Pb(SC_6F_4-4-H)$_2$] (56.9 mg, 0.1 mmol) in acetone (20 mL). Yield 90.1%. m.p. 180–181 °C. ^1H NMR (300 MHz, $CDCl_3$), δ 8.1–6.6 (m, Ph, 16H), 4.1–3.2 (br, s, CH_2, 2H), 2.88 (br, s, CH_3, 6H); $^{31}P\{^1H\}$ NMR (121 MHz, $CDCl_3$), δ 20.88 (s, P); $^{19}F\{^1H\}$ NMR (282 MHz, $CDCl_3$), δ −135.0 (m, $^3J_{Fo\text{-}Fm}$ = 25.0 Hz, *o*-F *trans* to N), −136.0 (m, $^3J_{Fo\text{-}Fm}$ = 25.0 Hz, *o*-F *trans* to P), −143.4 (m, $^3J_{Fm\text{-}Fp}$ = 25.0 Hz, *m*-F *trans* to N), −143.9 (m, $^3J_{Fm\text{-}Fp}$ = 25.0 Hz, *o*-F *trans* to P). Elem. Anal. Calculated for [$C_{33}H_{24}F_8NPPdS_2$] Calc. %:—C: 50.29, H: 3.07. Found %—C: 50.24, H: 3.08. MS-FAB$^+$ [M^+] = 787 *m*/*z*.

3.4.3. Synthesis of [Pd($Ph_2PC_6H_4$-2-(CH_2NMe_2)) (SC_6H_4-2-CF_3)$_2$] (**3**)

[Pd($Ph_2PC_6H_4$-2-(CH_2NMe_2))Cl_2] (50.0 mg, 0.1 mmol) in acetone (10 mL), a solution of [Pb(SC_6H_4-2-CF_3)$_2$] (56.1 mg, 0.1 mmol) in acetone (20 mL). Yield 82.2%. m.p. 203–204 °C. ^1H NMR (300 MHz, $CDCl_3$), δ 7.9–6.8 (m, Ph, 22H), 3.9–3.2 (br, s, CH_2, 2H), 2.87 (br, s, CH_3, 6H); $^{31}P\{^1H\}$ NMR (121 MHz, $CDCl_3$), δ 19.57 (s, P); $^{19}F\{^1H\}$ NMR (282 MHz, $CDCl_3$), δ −61.99 (s, F *trans* to N), −63.11 (s, F *trans* to P). Elem. Anal. Calculated for [$C_{35}H_{30}F_6NPPdS_2$] Calc. %—C: 53.88, H: 3.88. Found %—C: 53.86, H: 3.86. MS-FAB$^+$ [M^+] = 779 *m*/*z*.

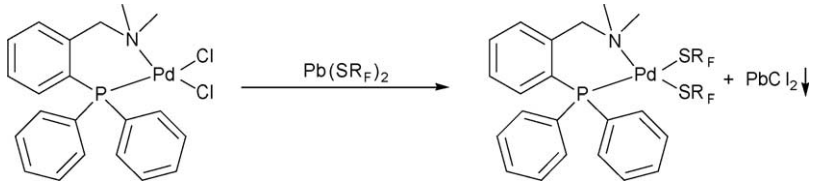

Scheme 3. Metathesis reactions for the synthesis of the complexes [Pd($Ph_2PC_6H_4$-2-(CH_2NMe_2))(SR_F)$_2$].

3.4.4. Synthesis of [Pd(Ph$_2$PC$_6$H$_4$-2-(CH$_2$NMe$_2$))(SC$_6$H$_4$-4-F)$_2$] (**4**)

[Pd(Ph$_2$PC$_6$H$_4$-2-(CH$_2$NMe$_2$))Cl$_2$] (50.0 mg, 0.1 mmol) in acetone (10 mL), a solution of [Pb(SC$_6$H$_4$-4-F)$_2$] (46.1 mg, 0.1 mmol) in acetone (20 mL). Yield 30.2%. m.p. 249–250 °C. ^{1}H NMR (300 MHz, CDCl$_3$), δ 7.9–6.6 (m, Ph, 22H), 3.9–3.8 (br, s, CH$_2$, 2H), 3.2–2.6 (br, s, CH$_3$, 6H); ^{31}P{^{1}H} NMR (121 MHz, CDCl$_3$), δ 20.97 (s, P); ^{19}F{^{1}H} NMR (282 MHz, CDCl$_3$), δ −112.64 (s, F *trans* to N), −118.98 (s, F *trans* to P). Elem. Anal. Calculated for [C$_{33}$H$_{30}$F$_2$NPPdS$_2$] Calc. %—C: 58.28, H: 4.45. Found %—C: 58.26, H: 4.46. MS-FAB$^+$ [M^+] = 679 *m*/*z*.

3.4.5. Synthesis of [Pd(Ph$_2$PC$_6$H$_4$-2-(CH$_2$NMe$_2$))(SC$_6$H$_4$-2-F)$_2$] (**5**)

[Pd(Ph$_2$PC$_6$H$_4$-2-(CH$_2$NMe$_2$))Cl$_2$] (50.0 mg, 0.1 mmol) in acetone (10 mL), a solution of [Pb(SC$_6$H$_4$-3-F)$_2$] (46.1 mg, 0.1 mmol) in acetone (20 mL). Yield 49.5%. m.p. 240–241 °C. ^{1}H NMR (300 MHz, CDCl$_3$), δ 7.7–6.5 (m, Ph, 22H), 3.9–3.2 (br, s, CH$_2$, 2H), 3.1–2.6 (br, s, CH$_3$, 6H); ^{31}P{^{1}H} NMR (121 MHz, CDCl$_3$), δ 20.57 (s, P); ^{19}F{^{1}H} NMR (282 MHz, CDCl$_3$), δ −103.5 (s, F *trans* to N), −109.1 (s, F *trans* to P). Elem. Anal. Calculated for [C$_{33}$H$_{30}$F$_2$NPPdS$_2$] Calc. %—C: 58.28, H: 4.45. Found %—C: 58.29, H: 4.50. MS-FAB$^+$ [M^+] = 679 *m*/*z*.

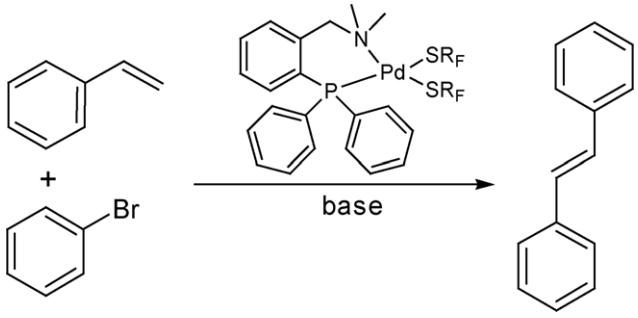

Scheme 4. The palladium catalyzed Heck coupling reaction using [Pd(Ph$_2$PC$_6$H$_4$-2-(CH$_2$NMe$_2$))(SR$_F$)$_2$] as catalyst.

3.5. General procedure for the catalytic reactions

A DMF solution (5 mL) of 50.0 mmol of bromobenzene, 60.0 mmol of styrene, and the prescribed amount of catalyst was introduced into a Schlenk tube in the open air. The tube was charged with a magnetic stir bar and an equimolar amount of base, sealed, and fully immersed in a 120 °C silicon oil bath. After the prescribed reaction time (2 h), the mixture was cooled to room temperature and the organic phase was analyzed by gas chromatography (GC/FID, GC–MS). A Varian Saturn 3 with DB-5 capillary column (30.0 m) was used for quantitative GC analysis (Scheme 4).

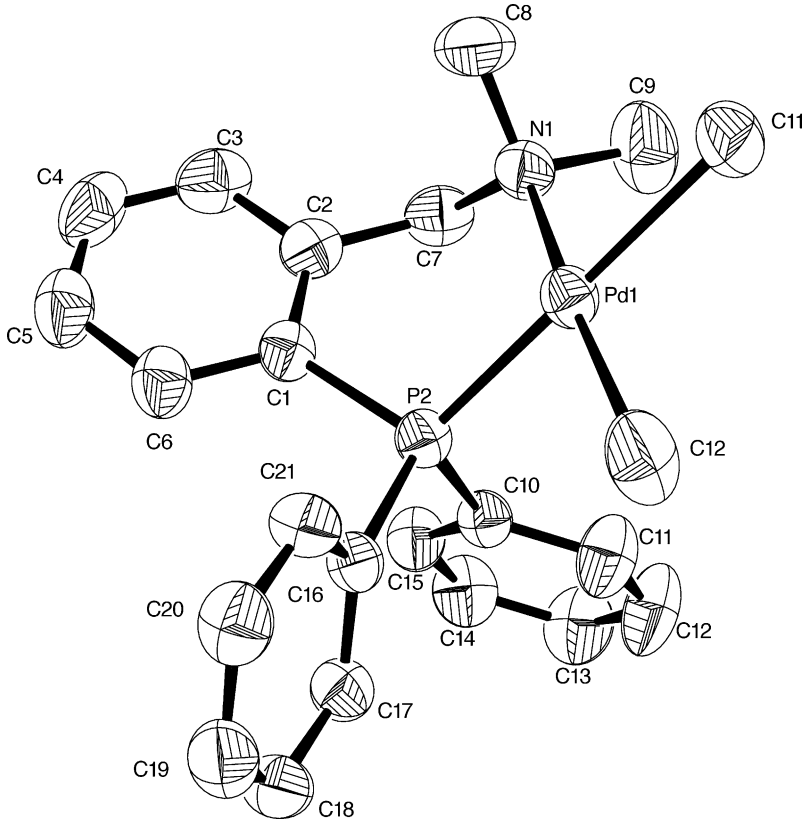

Fig. 3. An ORTEP representation of the structure of [Pd(Ph$_2$PC$_6$H$_4$-2-(CH$_2$NMe$_2$))(Cl)$_2$] (**1**) at 50% probability showing the atom labeling scheme.

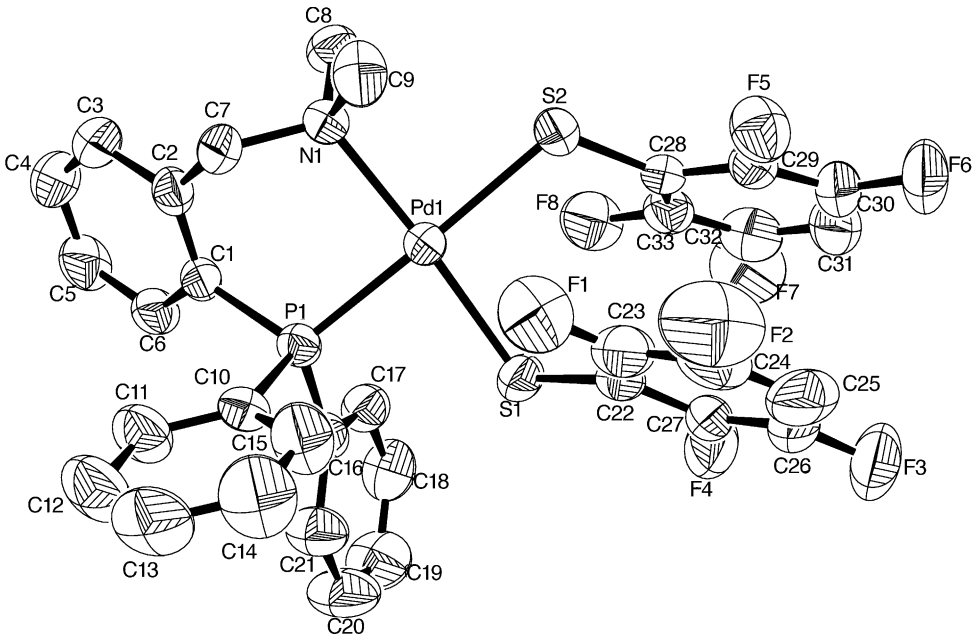

Fig. 4. An ORTEP representation of the structure of [Pd($Ph_2PC_6H_4$-2-(CH_2NMe_2))(SC_6F_4-4-H)$_2$] (**3**) at 50% probability showing the atom labeling scheme.

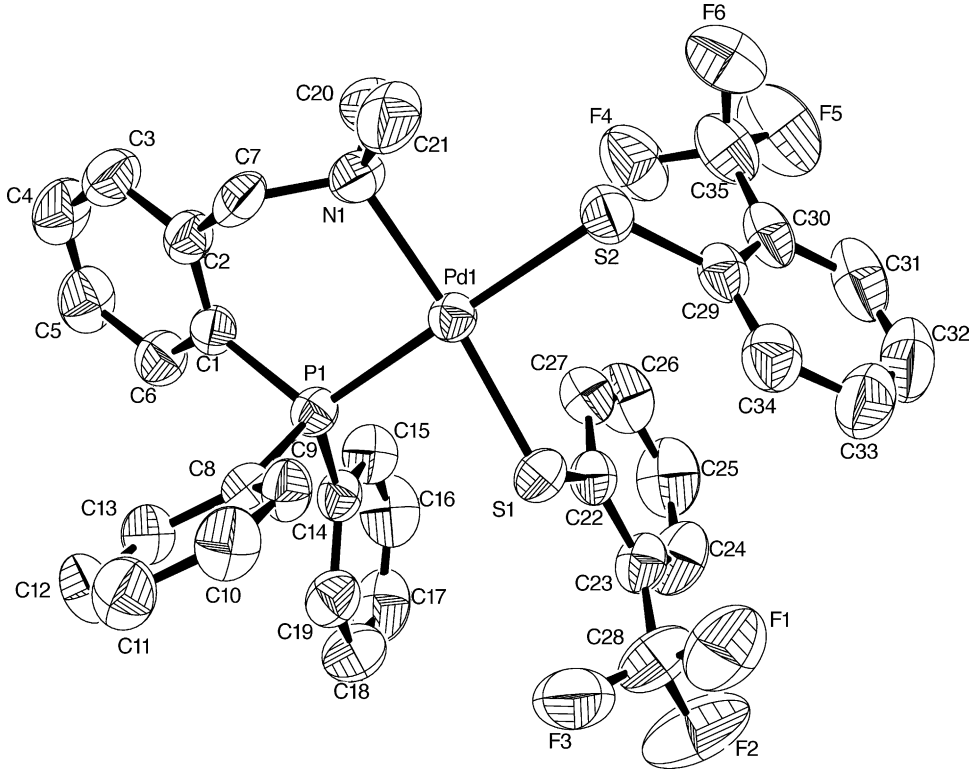

Fig. 5. An ORTEP representation of the structure of [Pd($Ph_2PC_6H_4$-2-(CH_2NMe_2))(SC_6H_4-2-CF_3)$_2$] (**4**) at 50% probability showing the atom labeling scheme.

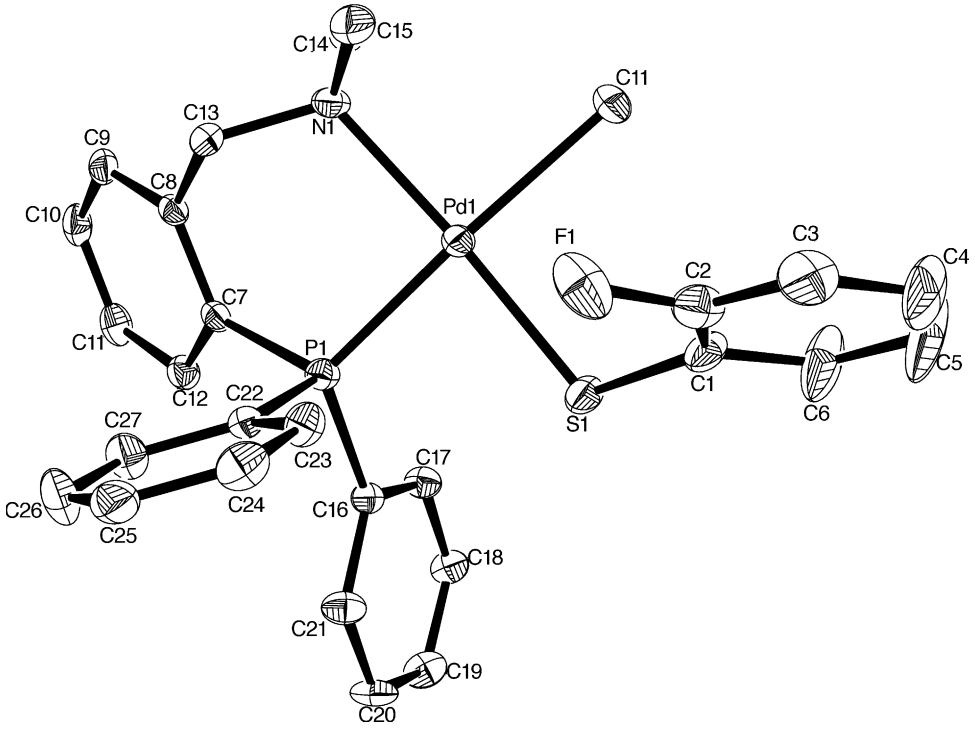

Fig. 6. An ORTEP representation of the structure of [Pd($Ph_2PC_6H_4$-2-(CH_2NMe_2))(Cl)(SC_6H_4-2-F)] (**7**) at 50% probability showing the atom labeling scheme.

*3.6. Data collection and refinement for [Pd($Ph_2PC_6H_4$-2-(CH_2NMe_2))($Cl)_2$] (**1**), [Pd($Ph_2PC_6H_4$-2-(CH_2NMe_2))(SC_6F_4-4-H)$_2$] (**3**), [Pd($Ph_2PC_6H_4$-2-(CH_2NMe_2))(SC_6H_4-2-CF_3)$_2$] (**4**), [Pd($Ph_2PC_6H_4$-2-(CH_2NMe_2))(Cl)(SC_6H_4-2-F)] (**7**)*

Crystalline red-orange prisms for **1**, **3**, **4** and **7** were grown independently by slow evaporation of CH_2Cl_2/MeOH solvent systems, and mounted on glass fibers. In all cases, the X-ray intensity data were measured at 293 or 291 K on a Bruker SMART APEX CCD-based X-ray diffractometer system equipped with a Mo-target X-ray tube ($\lambda = 0.71073$ Å). The detector was placed at a distance of 4.837 cm from the crystals in all cases. A total of 1800 frames were collected with a scan width of 0.3° in ω and an exposure time of 10 s/frame. The frames were integrated with the Bruker SAINT software package [12] using a narrow-frame integration algorithm. The integration of the data was done using a monoclinic unit cell in all cases, except for complex **1**, where an orthorhombic cell was used to yield a total of 32875, 25976, 26646 and 35358 reflections for **1**, **3**, **4** and **7** respectively to a maximum 2θ angle of 50.00° (0.93 Å resolution), of which 3722 (**1**), 5654 (**3**), 5879 (**4**) and 9363 (**7**) were independent. Analysis of the data showed in all cases negligible decays during data collections. The structures were solved by Patterson method using SHELXS-97 [13] program. The remaining atoms were located via a few cycles of least squares refinements and difference Fourier maps, using the space group *Pbca* with $Z = 8$ for **1**, $P2_1/c$ with $Z = 4$ for **3** and **7** and $P2_1/n$ with $Z = 4$ for **3**. Hydrogen atoms were input at calculated positions, and allowed to ride on the atoms to which they are attached. Thermal parameters were refined for hydrogen atoms on the phenyl groups using a Ueq = 1.2 Å to precedent atom in all cases. For all complexes, the final cycle of refinement was carried out on all non-zero data using SHELXL-97 [13] and anisotropic thermal parameters for all non-hydrogen atoms. The details of structure determinations are given in Table 1 and selected bond lengths (Å) and angles (°) are given in Table 2. Numbering of atoms is shown in Figs. 3–6 respectively (ORTEP) [14].

4. Supplementary material

Supplementary data for complexes **1**, **3**, **4** and **7** have been deposited at the Cambridge Crystallographic Data Centre. Copies of this information are available free of charge on request from The Director, CCDC, 12 Union Road, Cambridge, CB21EZ, UK (Fax: +44-1223-336033; e-mail: deposit@ccdc.cam.ac.uk or www: http://www.ccdc.cam.ac.uk) quoting the deposition numbers CCDC 256222 trough 256225.

Acknowledgements

JGF-A would like to thank CONACYT for financial support. We would like to thank Chem. Eng. Luis Velasco Ibarra, M.Sc. Francisco Javier Pérez Flores, QFB. Ma del Rocío Patiño and Ma. de las Nieves Zavala for their invaluable

help in the running of the FAB$^+$-Mass, IR and $^{19}F\{^1H\}$ spectra respectively. The support of this research by CONACYT (J41206-Q) is gratefully acknowledged.

References

[1] B. Cornils, W.A. Herrmann (Eds.), Applied Homogeneous Catalysis with Organometallic Compounds, vol. 2, Wiley–VCH/Verlag GmbH, Federal Republic of Germany, 2002, Chapter 3.
[2] I.P. Beletskaya, A.V. Cheprakov, Chem. Rev. 100 (2000) 3009.
[3] A.M. Rouhi, Chem. Eng. News 82 (2004) 49.
[4] (a) C.S. Stone, D.D. Weinberger, C.A. Mirkin, Prog. Inorg. Chem. 48 (1999) 233;
(b) P. Braunstein, F. Naud, Angew. Chem. Int. Ed. Engl. 40 (2001) 680.
[5] (a) L.L. Maisela, A.M. Crouch, J. Darkwa, I.A. Guzei, Polyhedron 20 (2001) 3189;
(b) O. Crespo, F. Canales, M.C. Gimeno, P.G. Jones, A. Laguna, Organometallics 18 (1999) 3142;
(c) D.-Y. Noh, E.-M. Seo, H.-J. Lee, H.-Y. Jang, M.-G. Choi, Y.H. Kim, J. Hong, Polyhedron 20 (2001) 1939;
(d) V.D. de Castro, G.M. de Lima, A.O. Porto, H.G.L. Siebald, J.D. de Souza Filho, J.D. Ardisson, J.D. Ayala, G. Bombieri, Polyhedron 23 (2004) 63;
(e) T.F. Baumann, J.W. Sibert, M.M. Olmstead, A.G.M. Barrett, B.M. Hoffman, J. Am. Chem. Soc. 116 (1994) 2639.
[6] J.R. Dilworth, J. Hu, Adv. Inorg. Chem. 40 (1993) 411.
[7] (a) D. Morales-Morales, R. Redón, Y. Zheng, J.R. Dilworth, Inorg. Chim. Acta 328 (2002) 39;
(b) D. Morales-Morales, C. Grause, K. Kasaoka, R. Redón, R.E. Cramer, C.M. Jensen, Inorg. Chim. Acta 300–302 (2000) 958;
(c) D. Morales-Morales, R. Redón, C. Yung, C.M. Jensen, Chem. Commun. (2000) 1619;
(d) D. Morales-Morales, R. Redón, Z. Wang, D.W. Lee, C. Yung, K. Magnuson, C.M. Jensen, Can. J. Chem. 79 (2001) 823;
(e) D. Morales-Morales, R.E. Cramer, C.M. Jensen, J. Organomet. Chem. 654 (2002) 44;
(f) X. Gu, W. Chen, D. Morales-Morales, C.M. Jensen, J. Mol. Catal. A 189 (2002) 119;
(g) J.R. Dilworth, P. Arnold, D. Morales, Y.L. Wong, Y. Zheng, The Chemistry and Applications of Complexes with Sulphur Ligands, Modern Coordination Chemistry. The Legacy of Joseph Chatt, Royal Society of Chemistry, Cambridge, UK, 2002, p. 217;
(h) D. Morales-Morales, S. Rodríguez-Morales, J.R. Dilworth, A. Sousa-Pedrares, Y. Zheng, Inorg. Chim. Acta 332 (2002) 101;
(i) V. Gómez-Benítez, S. Hernández-Ortega, D. Morales-Morales, Inorg. Chim. Acta 346 (2003) 256;
(j) D.W. Lee, C.M. Jensen, D. Morales-Morales, Organometallics 22 (2003) 4744;
(k) V. Gómez-Benítez, S. Hernández-Ortega, D. Morales-Morales, J. Mol. Struct. 689 (2004) 137;
(l) D. Morales-Morales, R. Redón, C. Yung, C.M. Jensen, Inorg. Chim. Acta 357 (2004) 2953;
(m) C. Herrera-Álvarez, V. Gómez-Benítez, R. Redón, J. García-Alejandre, S. Hernández-Ortega, R.A. Toscano, D. Morales-Morales, J. Organomet. Chem. 689 (2004) 2464;
(n) G. Ríos-Moreno, R.A. Toscano, R. Redón, H. Nakano, Y. Okuyama, D. Morales-Morales, Inorg. Chim. Acta 358 (2005) 303.
[8] D. Cruz-Garritz, J.A. Chamizo, M. Cruz, H. Torrens, Rev. Soc. Quim. Mex. 33 (1989) 18.
[9] (a) L.S. Reddy, A. Nangia, V.M. Lynch, Cryst. Growth Des. 4 (2004) 89;
(b) D.B. Fox, R. liantonio, P. Metrangolo, T. Pilati, G. Resnati, J. Fluor. Chem. 125 (2004) 271.
[10] D. Drew, J.R. Doyle, Inorg. Synth. 28 (1990) 348.
[11] M.E. Peach, Can. J. Chem. 46 (1968) 2699.
[12] A.X.S. Bruker, SAINT Software Reference Manual, Madison, WI, 1998.
[13] G.M. Sheldrick, SHELXTL NT Version 6.10, Program for Solution and Refinement of Crystal Structures, University of Göttingen, Germany, 2000.
[14] L.J. Farrugia, ORTEP-3 for Windows, J. Appl. Crystallogr. 30 (1997) 565.